

The Paschen-Back Effect. I. *L-S* Coupling; the ${}^3P^3D$ Multiplets of Zn and Cd

J. B. GREEN AND D. E. GRAY, *Mendenhall Laboratory of Physics, Ohio State University*

(Received December 16, 1933)

Darwin's calculations for Zeeman effect are applied to the Zn and Cd ${}^3P^3D$ multiplets. The frequencies and intensities thus calculated show very good agreement with the experimental values. A considerably smaller dis-

crepancy between experiment and older quantum theory is noted for the Cd than for the Zn as should be expected because of the much larger multiplet separation in the case of the former.

THE new quantum mechanics has been applied to the calculation of standard Zeeman effect at all field strengths by Heisenberg and Jordan,¹ and Darwin.² Intensity rules have been given by Kronig³ and Fowler.⁴ Mensing⁵ has applied these results to the cases of the ${}^2P^2D$ multiplet of Na and to the ${}^3P^3D$ multiplet of Mg. In these two cases the *D* separation is very much smaller than the separation of the *P* levels so that a very strong field for the *D* levels constitutes a weak field for the *P* levels. One of us⁶ has extended the application to the ${}^2P^2D$ multiplet of Cu and the ${}^3S^3P$ of Be and of Mg. The purpose of this paper is to extend further these calculations to the ${}^3P^3D$ multiplets as observed in the Zn and Cd spectra and compare the calculated frequencies and intensities with those observed experimentally. Homologous multiplets in these two spectra were chosen to obviate the necessity of changing the field strength and still be able to maintain resolved patterns.

The experimental investigations were made on the 21-foot concave grating set-up at Ohio State University. This set-up employs a 30,000 line concave grating in a Paschen-Runge type mounting. The magnet is of the Weiss type. With ferrocobalt pole tips 1 cm in diameter and a pole gap of about 3 mm, a field strength of 40,000 gauss is obtainable. The light source consists of a spark

discharge which takes place in vacuum between a brass wire and the knurled periphery of a revolving disk along which the wire rubbed.⁷ A plain brass disk was used to obtain the Zn spectrum and a similar disk having a rim of cadmium for the Cd spectrum. The field strength used was found by calculation from the observed separations of the Zn lines $\lambda 4722$ and $\lambda 4810$ whose patterns are accurately known.

Darwin² has developed the formula for the positions of the energy levels in a magnetic field of strength $\omega = eHh/4\pi m_0 C$:

$$\begin{aligned} & -a_{m_l-1, m_s+1} \beta (l - m_l + 1) (s + m_s + 1) \\ & + a_{m_l m_s} [W - \beta \cdot 2m_l m_s - \omega (m_l + 2m_s)] \\ & - a_{m_l+1, m_s-1} \beta (l + m_l + 1) (s - m_s + 1) = 0. \end{aligned}$$

Where m_l and m_s have their usual significance, β is a constant of the field free multiplet separation, ω is the field strength in cm^{-1} units and W gives the separation in cm^{-1} units of the component from the center of gravity of the multiplet. The a 's are numerical coefficients related to the intensities.

The procedure is to write the above equation for all permissible combinations of m_l and m_s to give a certain value of m where $m = m_l + m_s$. Each such set of equations forms a determinant whose solutions are the values of W for that particular value of m . The intensity formulae may be found in Darwin's work. The polarizing action of the grating makes it impossible to compare intensities of parallel components with perpendicular ones.

⁷ See description of vacuum source by Green and Loring in Phys. Rev. **43**, 459 (1933).

¹ Heisenberg and Jordan, Zeits. f. Physik **37**, 263 (1926).

² Darwin, Proc. Roy. Soc. **A115**, 1 (1927); also K. Darwin, Proc. Roy. Soc. **A118**, 264 (1928).

³ Kronig, Zeits. f. Physik **31**, 885 (1925).

⁴ Fowler, Phil. Mag. **1**, 1079 (1925).

⁵ Mensing, Zeits. f. Physik **39**, 24 (1926).

⁶ Green, Phys. Rev. **36**, 157 (1930).

TABLE I. *Zinc*.

Position of undisturbed line	Observed position in field	Calculated new theory (1)	Calculated old theory (2)	Obs. int.	Calc. int. (1)	Calc. int. (2)	Position of undisturbed line	Observed position in field	Calculated new theory (1)	Calculated old theory (2)	Obs. int.	Calc. int. (1)	Calc. int. (2)
(P_0-D_1)	-1.50	-1.58	-0.92	10	6.6	13.0	(P_2-D_1)	—	-4.95	-4.60	—	0.02	0.4
3282.326	-0.55 <i>p</i>	-0.59 <i>p</i>	0.00 <i>p</i>	22	23.2	26.0		—	-3.35	-2.76	—	0.02	0.2
30,457.45	0.58	0.57	0.92	12	12.6	13.0		—	-1.58	-0.92	—	0.2	0.1
(P_0-D_2)	-1.85	-1.80	fbdn	2	2.8	0	3345.940	—	-2.20 <i>p</i>	-1.84 <i>p</i>	—	0.6	0.4
forbidden	0.28 <i>p</i>	0.26 <i>p</i>	fbdn	2	3.6	0	29,878.41	—	-0.59 <i>p</i>	0.00 <i>p</i>	—	0.2	0.6
	2.15	2.21	fbdn	1	0.9	0		—	1.19 <i>p</i>	1.84 <i>p</i>	—	0.2	0.4
								2.22	0.57	0.92	—	0.6	0.1
(P_0-D_3)	—	-2.60	fbdn	—	0.2	0		4.04	2.17	2.76	2	1.4	0.2
forbidden	—	-0.13 <i>p</i>	fbdn	—	0.04	0			3.94	4.60	2	1.6	0.4
	—	2.28	fbdn	—	0.02	0							
	-3.28	-3.35	-2.76	4	2.2	5.0			-3.29	-3.38	—	1.4	2.0
(P_1-D_1)	—	-1.41	-0.92	—	0.1	5.0		-2.50	-2.48	-2.76	2	1.6	3.0
3302.948	-2.11 <i>p</i>	-2.20 <i>p</i>	-1.84 <i>p</i>	4	3.8	10.0		—	-1.78	-2.14	—	0.8	3.0
30,267.30	-0.54 <i>p</i>	-0.60 <i>p</i>	fbdn	4	4.0	0		—	-1.71	-1.54	—	0.4	2.0
	1.28 <i>p</i>	1.19 <i>p</i>	1.84 <i>p</i>	22	22.0	10.0	(P_2-D_2)	-1.37 <i>p</i>	-1.38 <i>p</i>	-1.22 <i>p</i>	6	4.8	8.0
	0.59	0.56	0.92	6	8.2	5.0	3345.572	—	-0.53 <i>p</i>	-0.62 <i>p</i>	—	0.02	2.0
	2.22	2.17	2.76	6	7.4	5.0	29,881.70	0.26 <i>p</i>	0.28 <i>p</i>	fbdn	4	2.2	0
								0.99 <i>p</i>	0.98 <i>p</i>	0.62 <i>p</i>	24	6.8	2.0
									1.05 <i>p</i>	1.22 <i>p</i>		12.6	8.0
	-2.45	-2.47	-2.76	4	5.6	3.0		1.43	1.38	1.54	6	4.0	2.0
	-1.73	-1.78	-2.14	25	12.8	9.0		2.21	2.23	2.14	4	4.8	3.0
(P_1-D_2)	-0.49 <i>p</i>	-0.52 <i>p</i>	-0.62 <i>p</i>	20	24.2	18.0		3.09	3.04	2.76	4	3.6	3.0
3302.589	0.30 <i>p</i>	0.29 <i>p</i>	0.00 <i>p</i>	14	19.0	24.0		3.71	3.74	3.78	2	1.4	2.0
30,270.59	1.01 <i>p</i>	0.99 <i>p</i>	0.62 <i>p</i>	6	4.8	18.0							
	1.41	1.39	1.54	20	17.8	18.0							
	2.24	2.23	2.14	6	5.0	9.0							
	—	3.05	2.76	—	0.6	3.0							
	—	-2.52	fbdn	—	0.2	0	(P_2-D_3)	—	-2.83	-3.06	—	2.4	1.6
	—	-2.23	fbdn	—	0.02	0	3345.023	-2.48	-2.48	-2.76	6	6.6	4.8
	—	-2.00	fbdn	—	0.6	0	29,886.60	-2.17	-2.19	-2.46	10	11.8	9.6
	—	-0.05 <i>p</i>	fbdn	—	0.8	0		-1.94	-1.98	-2.14	14	17.8	16.0
(P_1-D_3)	—	0.29 <i>p</i>	fbdn	—	1.2	0		-1.84	-1.84	-1.84	20	24.0	24.0
forbidden	—	0.59 <i>p</i>	fbdn	—	0.8	0		-0.47 <i>p</i>	-0.48 <i>p</i>	-0.62 <i>p</i>	20	19.2	16.0
	2.27	2.35	fbdn	4	4.8	0		-0.07 <i>p</i>	-0.07 <i>p</i>	-0.30 <i>p</i>	24	27.2	25.6
	—	2.75	fbdn	—	0.4	0		0.28 <i>p</i>	0.28 <i>p</i>	0.00 <i>p</i>	20	20.0	28.8
	—	3.12	fbdn	—	0.2	0		0.58 <i>p</i>	0.57 <i>p</i>	0.30 <i>p</i>	16	20.8	25.6
								0.82 <i>p</i>	0.79 <i>p</i>	0.62 <i>p</i>	8	11.4	16.0
								1.80	1.84	1.84	16	24.0	24.0
								2.30	2.29	2.14	14	14.0	16.0
								2.72	2.69	2.46	6	6.0	9.6
								3.02	3.04	2.76	4	3.0	4.8
								—	3.33	3.06	—	0.8	1.6

For each complete set of data, it was necessary to take four sets of plates. The first was a zinc arc in air together with an iron comparison spectrum, to determine the absolute wave-lengths of the lines of the multiplets. The second set was the complete Zeeman pattern without using any polarizing device. The third set was the perpendicularly polarized components together with the arc in air. This gives the absolute position of the perpendicular components. The fourth set was the parallel polarized components alone. This enabled us to separate out any overlapping of parallel and perpendicular components in the complete pattern of the second set and, through the measurements of the second and third sets, to determine the absolute positions of the parallel components.

$^3P^3D$ MULTIPLET OF ZN

The $^3P^3D$ multiplet of Zn consists of six lines: $\lambda\lambda 3345.9, 3345.6, 3345.0, 3302.9, 3302.6, 3282.3$. For the 3P levels $\beta = 579.04/6 = 96.51 \text{ cm}^{-1}$. For the 3D levels $\beta = 8.19/10 = 0.819 \text{ cm}^{-1}$. The field

strength $\omega = 1.85 \text{ cm}^{-1}$. The numerical results are given in Table I. The position of each component is stated in terms of its separation from the field free line in cm^{-1} units. Negative separations indicate frequencies less than that of the parent line. The observed intensities are estimated.

It will be noted that in all but two or three cases the new theory gives much better agreement with the observed positions of the lines than the old. The two or three components for which the positions calculated by the old and new theories fit equally well are cases of weak lines. All cases of unobserved components are lines whose intensities calculate to be very small on the newer theory.

Components which the older theory entirely forbids are especially interesting. The Δj selection rule forbids all components of $P_1-D_3, P_0-D_3,$ and P_0-D_2 . One component of P_1-D_3 and all components of P_0-D_2 are observed and check with the Darwin theory. The balance of the P_1-D_3 group and all of the P_0-D_3 lines which are not observed are calculated to have very small

TABLE II. *Cadmium.*

Position of undisturbed line	Observed position in field	Calculated new theory (1)	Calculated old theory (2)	Obs. int.	Calc. int. (1)	Calc. int. (2)	Position of undisturbed line	Observed position in field	Calculated new theory (1)	Calculated old theory (2)	Obs. int.	Calc. int. (1)	Calc. int. (2)
(P_0-D_1) 3403.653 29,371.76	-1.05	-1.05	-0.91	13	14.0	13.0	(P_2-D_1) 3614.4 27,658.96	—	-4.67	-4.55	—	0.3	0.4
	-0.19 <i>p</i>	-0.15 <i>p</i>	0.00 <i>p</i>	20	21.0	26.0		—	-2.88	-2.73	—	0.03	0.2
	0.81	0.82	0.91	13	14.0	13.0		—	-1.05	-0.91	—	0.0	0.1
(P_0-D_2) forbidden	—	-2.05	fbdn	—	0.1	0	—	—	-1.93 <i>p</i>	-1.82 <i>p</i>	—	0.7	0.4
	—	0.06 <i>p</i>	fbdn	—	0.1	0	—	—	-0.15 <i>p</i>	0.00 <i>p</i>	—	0.6	0.6
(P_0-D_3) forbidden	—	2.16	fbdn	—	0.1	0	—	—	1.68 <i>p</i>	1.82 <i>p</i>	—	0.3	0.4
	—	—	—	—	—	—	—	—	0.80	0.91	—	0.3	0.1
(P_1-D_1) 3467.656 28,829.59	—	-2.36	fbdn	—	0.0	0	—	—	2.58	2.73	—	0.6	0.2
	—	0.09 <i>p</i>	fbdn	—	0.0	0	—	—	4.42	4.55	—	0.8	0.4
	—	2.50	fbdn	—	0.0	0	—	—	—	—	—	—	—
(P_1-D_2) 3467.656 28,829.59	-2.90	-2.88	-2.73	4	4.0	5.0	(P_2-D_2) 3612.875 27,670.63	-3.32	-3.30	-3.34	2	2.0	2.0
	-1.10	-1.05	-0.91	4	3.3	5.0		-2.64	-2.67	-2.73	3	2.6	3.0
	-1.90 <i>p</i>	-1.93 <i>p</i>	-1.82 <i>p</i>	6	7.1	10.0		-2.04	-2.05	-2.12	3	2.6	3.0
	0.82	0.15 <i>p</i>	fbdn	—	0.0	0		-1.57	-1.57	-1.52	2	1.3	2.0
	2.55	1.68 <i>p</i>	1.82 <i>p</i>	10	13.3	10.0		-1.23 <i>p</i>	-1.25 <i>p</i>	-1.21 <i>p</i>	5	6.5	8.0
(P_1-D_2) 3466.201 28,841.70	0.82	0.80	0.91	8	7.7	5.0	—	-0.55 <i>p</i>	-0.57 <i>p</i>	-0.61 <i>p</i>	1	1.3	2.0
	2.10	2.58	2.73	8	6.0	5.0	0.68 <i>p</i>	0.68 <i>p</i>	0.61 <i>p</i>	2	3.3	2.0	
	-2.62	-2.67	-2.73	3	4.3	3.0	1.16 <i>p</i>	1.16 <i>p</i>	1.21 <i>p</i>	8	9.3	8.0	
	-2.05	-2.05	-2.12	10	10.8	9.0	1.42	1.48	1.52	2	2.7	2.0	
	-1.58	-1.57	-1.52	17	18.0	18.0	2.09	2.16	2.12	5	3.3	3.0	
(P_1-D_3) forbidden	-0.57 <i>p</i>	-0.57 <i>p</i>	-0.61 <i>p</i>	20	21.0	18.0	2.76	2.79	2.73	5	3.3	3.0	
	0.09 <i>p</i>	0.06 <i>p</i>	0.00 <i>p</i>	20	23.4	24.0	3.38	3.41	3.34	3	2.0	2.0	
	0.68 <i>p</i>	0.68 <i>p</i>	0.61 <i>p</i>	17	14.7	18.0	—	—	—	—	—	—	—
	1.46	1.48	1.52	17	18.0	18.0	-2.96	-2.96	-3.13	2	2.0	1.6	
	2.10	2.16	2.12	7	7.3	9.0	-2.63	-2.64	-2.73	5	4.7	4.8	
2.79	2.79	2.73	1	2.0	3.0	-2.34	-2.35	-2.43	8	10.0	9.6		
(P_1-D_3) forbidden	—	-2.64	fbdn	—	0.03	0	-2.08	-2.07	-2.12	14	16.7	16.0	
	—	-2.36	fbdn	—	0.3	0	-1.80	-1.82	-1.82	20	24.0	24.0	
	—	-2.07	fbdn	—	0.1	0	-0.56 <i>p</i>	-0.57 <i>p</i>	-0.62 <i>p</i>	14	17.3	16.0	
	—	-2.03 <i>p</i>	fbdn	—	0.1	0	-0.21 <i>p</i>	-0.23 <i>p</i>	-0.31 <i>p</i>	24	26.7	25.6	
	—	0.09 <i>p</i>	fbdn	—	0.1	0	0.09 <i>p</i>	0.09 <i>p</i>	0.00 <i>p</i>	24	28.6	28.8	
	—	0.37 <i>p</i>	fbdn	—	0.1	0	0.38 <i>p</i>	0.37 <i>p</i>	0.31 <i>p</i>	20	24.6	25.6	
	—	2.16	fbdn	—	0.1	0	0.69 <i>p</i>	0.66 <i>p</i>	0.62 <i>p</i>	16	14.7	16.0	
	—	2.50	fbdn	—	0.03	0	1.84	1.82	1.82	24	24.0	24.0	
	—	2.82	fbdn	—	0.03	0	2.14	2.16	2.12	16	15.3	16.0	
	—	—	—	—	—	—	2.46	2.49	2.43	9	8.7	9.6	
—	—	—	—	—	—	2.80	2.82	2.73	5	4.0	4.8		
—	—	—	—	—	—	3.07	3.10	3.13	1	1.3	1.6		

intensities. The older theory also forbids any transition for which $m=0 \rightarrow m=0$ when Δj equal zero. Examples of this are seen in the center parallel components of P_2-D_2 and P_1-D_1 . In both cases lines are observed and show good agreement. The components at 0.98 and 1.05 in the P_2-D_2 group are unresolved and the line observed at 0.99 shows an intensity comparable with the sum of the two. A similar case occurs in the line observed at -1.73 in the P_1-D_2 group.

$^3P^3D$ MULTIPLY OF CD

Results of similar investigation of the same multiplet in Cd are shown in Table II and Figs. 1b and 2b. The six lines of this multiplet occur at $\lambda\lambda 3614.4, 3612.9, 3610.5, 3467.7, 3466.2, 3403.7$. For the 3P levels $\beta = 1712.8/6 = 285.47 \text{ cm}^{-1}$ and for the 3D levels equals $29.8/10 = 2.98 \text{ cm}^{-1}$. The field strength $\omega = 1.82 \text{ cm}^{-1}$.

There will be noted in these results a much closer agreement between old and new theory than in the previous case. This is to be expected since the constants of multiplet separation here are much larger, some 3.5 times as large for the

3D levels and 3 times as large for the 3P . In this case, then, the field of approximately the same strength as before comes nearer being a weak field, i.e., one in which the multiplet separation is much greater than the normal Zeeman separation.

However, here also in most cases the new theory shows better agreement with observation. For seven lines the two theories give about equal agreement and for two—the 2.10 component of P_1-D_2 and the 2.09 component of P_2-D_2 —the older theory checks slightly better with experiment.

No check can be made here on forbidden lines since all lines forbidden by old theory have a small calculated intensity by new theory and none were observed in these comparatively short exposures.

CONCLUSIONS

The intervals of the 3D levels of both Zn and Cd are extremely close to 3 : 2 and the 1D levels are sufficiently far away so that we may assume that we have cases of Russell-Saunders ($L-S$) coupling. The experimental evidence of the present paper

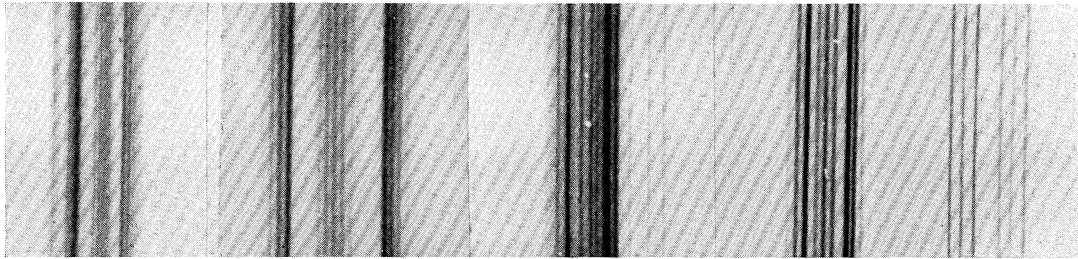


Fig. 1a

Fig. 1b

Fig. 2a

Fig. 2b

FIG. 1a. Zn 3345 $^3P_2 - ^3D_2$ (second order)

FIG. 1b. Cd 3610 $^3P_2 - ^3D_2$ (third order)

FIG. 2a. Zn 3302-3 $^3P_1 - ^3D_2$ and $^3P_1 - ^3D_1$ (second order)

FIG. 2b. Cd 3466-8 $^3P_1 - ^3D_2$ and $^3P_1 - ^3D_1$ (third order)

The figures show clearly that the first evidence of the beginning Paschen-Back effect is a distortion of intensities, as shown in the case of the cadmium lines, while with greatly increased field strengths (relative to the multiplet separations) the positions of the components are so badly distorted as almost to destroy the symmetry of the pattern.

shows that the Darwin theory is quite adequate for the calculation of the positions and intensities of the Zeeman components. The first noticeable effect of the increasing magnetic field is a distortion of intensities. This is the case with Cd. It is not until the field becomes quite strong that the field distorts the positions of the lines very markedly. (See Figs. 1 and 2.)

In the spectrum of mercury, $L-S$ coupling is practically completely destroyed and the Darwin theory is no longer adequate for the explanation of the experimental evidence. The results for mercury will be published shortly.

The authors wish to thank Dr. R. A. Loring for his willing cooperation.

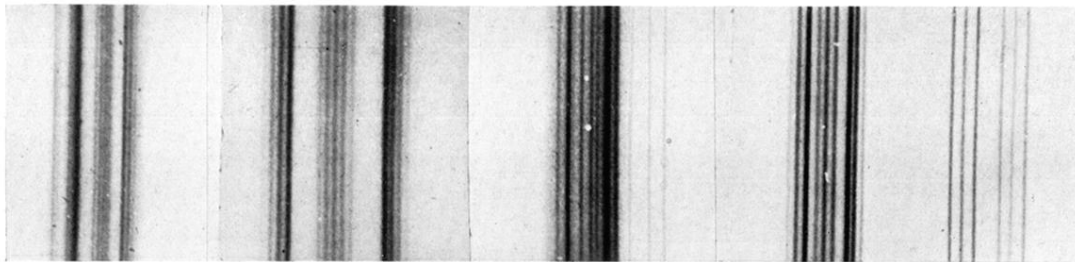


Fig. 1a

Fig. 1b

Fig. 2a

Fig. 2b

FIG. 1a. Zn 3345 ${}^3P_2-{}^3D_2$ (second order)

FIG. 1b. Cd 3610 ${}^3P_2-{}^3D_2$ (third order)

FIG. 2a. Zn 3302-3 ${}^3P_1-{}^3D_2$ and ${}^3P_1-{}^3D_1$ (second order)

FIG. 2b. Cd 3466-8 ${}^3P_1-{}^3D_2$ and ${}^3P_1-{}^3D_1$ (third order)

The figures show clearly that the first evidence of the beginning Paschen-Back effect is a distortion of intensities, as shown in the case of the cadmium lines, while with greatly increased field strengths (relative to the multiplet separations) the positions of the components are so badly distorted as almost to destroy the symmetry of the pattern.